Dual-Energy X-Ray Imaging: Benefits and Limits

Véronique REBUFFEL and Jean-Marc DINTEN, CEA-LETI, Grenoble, France

Abstract. Both in radiographic and tomographic mode, conventional X-ray imaging provides information about the examined object which is not sufficient to characterize it precisely. Dual-energy X-ray technique, which consists in combining two radiographs acquired at two distinct energies, allows to obtain both density and atomic number, thus to provide information about material composition, or at least to improve image contrast. Available systems usually perform energetic separation at source level, but separation at detector level is also possible for linear detectors, especially those devoted to translating objects control.
Dual-energy equations can be easily written and solved for monochromatic energy spectra and perfect detectors, but become complex when considering realistic spectra, detector sensitivity, and system non–linearity. A decomposition into material basis, using experimental dual-material calibration, allows to solve an approximated system, while getting free of beam hardening and other disturbances.
More generally, we analyze the various problems to be solved before benefiting from dual-energy approach, and propose available solutions. We evaluate influence of noise on results accuracy, that strongly influences materials distinguishability. We review the aspects to optimize when considering a specific industrial problem: choice of energy spectra, of materials basis, method design. Numerical simulation is an efficient tool for that optimal system design. Various industrial applications will be considered.

1. Introduction

Conventional X-ray imaging modality can provide a representation of the object under examination in terms of attenuation coefficient in case of tomographic mode, and of product of attenuation by material thickness, in radiographic mode. This information is not sufficient to characterize precisely the observed object. In the usual inspection energy range, the attenuation for X-ray radiation is a combination of two photon-matter interactions: the photo-electric effect and Compton scatter. The two interactions and their relative contribution to the total attenuation are energy dependant. Thus, measurements at two distinct energies should permit the separation of the attenuation into its basic components, which can be used to identify material, and finally to produce material-specific image. Another consequence could be to determine material thickness, or to produce more contrasted images. But as for any quantitative measurement, all disturbances have to be taken into account in order to assure that uncertainty on final result is not greater than required accuracy. In this article we first remind the principles of dual-energy technique, then we evaluate the various possible noise and disturbances. We detail the choices to be done when designing a dual-energy system and discuss about criteria to optimize this design. Considering a specific industrial problem, dual-energy techniques can be very helpful, or non convenient – our purpose is to give some guidelines to evaluate this interest.

First let us present the different modalities of dual-energy data acquisition. Notice that the two measures, *LE* and *HE* ones, have to be acquired in similar geometry in order to allow their numerical combination. A first approach consists in dual exposure technique. Two acquisitions are performed successively, the energy switch being realized by voltage tuning associated with the use of filters placed behind the generator. This method has been found to be efficient in terms of energy separation, but it assumes that the object is static. It can be implemented with a 2D detector, allowing an acquisition rate at the detector speed. The field dimension is limited, to 30x40 cm for the largest. Furthermore, the use of a 2D detector, either scintillator screen or more recent flat panel, induces influence of scatter, problematic for numerical accuracy. Typical applications can be found in medical domain. Dual-energy may also be implemented within a single exposure technique. Adapted detectors consist in two receptor layers separated by an intermediate filter. The front detector records the low-energy photons, while the back detector the high-energy ones. The two images are acquired simultaneously, allowing to inspect moving object. CR systems have been validated for medical field. Linear "sandwich-type" detectors are used in airport control, for the inspection of luggage on conveyor belts. Notice that a linear detector permits an efficient collimation, and can be as long as required. But the energy separation of single exposure technique is poor. Spectrometric detectors assuring narrow energy resolution are available today, in a linear array form only; they take benefit of the recent technologies of semiconductor as CdTe [1]. The energy accuracy can reach a few KeV. Notice that the extension to multi-energy technique can be envisaged only in successive exposure mode, or in single exposure mode but with spectroscopic detectors. Finally, a large range of technological solutions are available, the best choice should depend on the specific constraints of the considered problem.
In the follow up we use LE for Low Energy, and HE for High Energy.

2. Dual-energy physical concepts and methodology

2.1 Bi-chromatic model

If a monochromatic source emits a number of photons N_0, then the number of photons N imaging on a collimated detector of one pixel (linear response) after attenuation by a thickness T (cm) of an object of attenuation μ (cm^{-1}), is given by: $N = N_0 \exp(-\mu \cdot T)$.
The coefficient μ depends on the density of the material (ρ), on its chemical composition (effective atomic number Z), and on the energy E of the photons: $\mu = \rho \cdot \tau(E,Z)$ where τ is the mass attenuation of the material (cm2/g). For an inhomogeneous object, the product $\mu \cdot T (= \rho \cdot \tau \cdot T)$ has to be replaced by its integral along one ray $\tau \cdot \int \rho(l)\, dl$.
If we compute the log-measurement of the attenuation, we get: $m_E = -Log(N/N_0) = T \cdot \mu = T \cdot \rho \cdot \tau(E,Z)$, which is proportional to the thickness crossed by the x-ray. If the object is composed of several materials $m_E = \sum_{material\ i} T_i \cdot \rho_i \cdot \tau_i(E, Z_i)$

Let us now consider two materials 1 and 2. Two acquisitions at two distinct energies *LE* and *HE* then provide a linear system: $\begin{cases} m_{LE} = \mu_1^{LE} \cdot T_1 + \mu_2^{LE} \cdot T_2 \\ m_{HE} = \mu_1^{HE} \cdot T_1 + \mu_2^{HE} \cdot T_2 \end{cases}$ (1)

which can be easily solved as long as its determinant $\Delta = \mu_1^{LE} \cdot \mu_2^{HE} - \mu_1^{HE} \cdot \mu_2^{LE}$ is non null, which traduce the fact that chemical properties of the materials differ significantly. Examples of values of $\tau(E)$ are given in figure 1 for some materials.

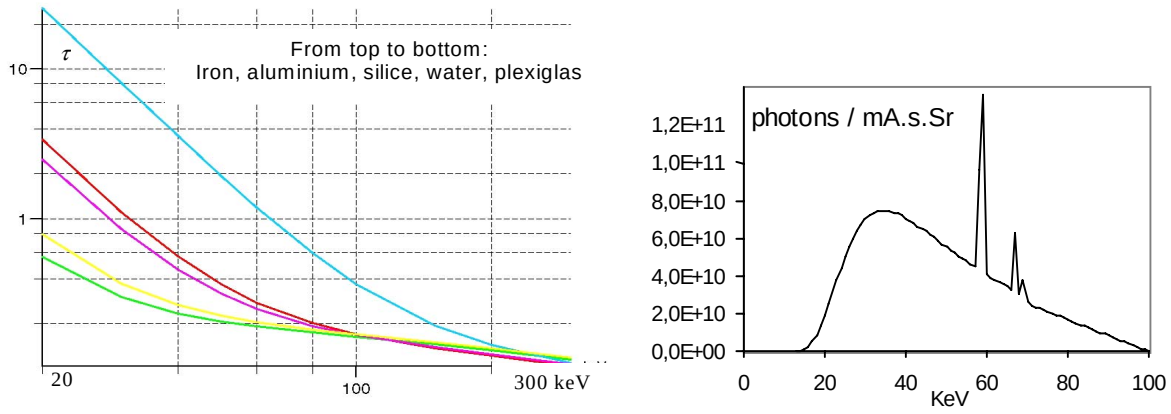

Figure 1: *(left)* Mass attenuation function for some materials, from 20 to 300 keV
(right) Model of spectrum, voltage 100 KV, tungsten anode, filtration 2 mm Al

2.2 Dual-material decomposition

The spectra of an X-ray tube is polychromatic (typical shape figure 1), inducing beam hardening effect. The log-measurement of attenuation for a spectrum in the energy range $[E_1, E_2]$ along a ray path *r* should be written:

$$m_{[E1,E2]}(r) = -Log\left(\int_{E1}^{E2} N_0^{'}(E)\cdot e^{-\sum_i T_i(r)\cdot\mu_i(E)}\,dE\right) \quad \text{with} \quad N_0^{'}(E) = \frac{D(E)\cdot N_0(E)}{\int_{E1}^{E2} D(E)\cdot N_0(E)\cdot dE}$$

where *D(E)* represents the detector efficiency. The relationship between attenuation measurement and material thickness is no more linear. Notice that we have not yet taken into account the scattering effect.

An important literature can be found on dual-energy techniques, from the initial works of Alvarez [2]. Most of the methods rely on the hypothesis that the attenuation coefficient can be decomposed linearly on a basis of two functions, depending only on energy of emitted photons, and corresponding to photo-electric and Compton effects - for instance $\mu(\rho, Z, E) = \rho Z^m \alpha(E) + \rho\beta(E)$. The resulting system presenting numerical instability and being difficult to calibrate, an alternative model which consists in decomposition on a material basis is often preferred [3]. The attenuation functions of two independent materials are then assumed to constitute a basis of the attenuation functions space. Thus, given materials named 1 and 2, we can write, for any material of characteristics (ρ, Z):

$$\mu(\rho, Z, E) = a_1(\rho, Z)\cdot\mu_1(E) + a_2(\rho, Z)\cdot\mu_2(E) \qquad (2)$$

the coefficients a_1 and a_2 being independent of energy.

The system representing the acquisitions at two distinct energies *LE* and *HE* is now:

$$\begin{cases} m_{LE}(r) = -Log\int_{E1_{LE}}^{E2_{LE}} N_{0LE}^{'}(E)\cdot e^{-\mu_1(E)\cdot A_1(r)-\mu_2(E)\cdot A_2(r)}dE \\ m_{HE}(r) = -Log\int_{E1_{HE}}^{E2_{HE}} N_{0_{HE}}^{'}(E)\cdot e^{-\mu_1(E)\cdot A_1(r)-\mu_2(E)\cdot A_2(r)}dE \end{cases}$$

where $A_1(r) = \sum_{mat\ i} T_i(r)\cdot a_1(\rho_i, Z_i)$ et $A_2(r) = \sum_{mat\ i} T_i(r)\cdot a_2(\rho_i, Z_i)$ represent the equivalent thickness of material 1 (resp.2) along ray r. Notice that this formalism is still convenient whatever the number of constituting materials *i* is.

Various approaches have been proposed to solve this non-linear system [4, 5, 6]. A commonly used one consists in modelling the inverse relationship by 2nd-order polynomial functions (sometimes the 3rd order is required [7]):

$$\begin{cases} A_1(r) = \alpha_0 + \alpha_1 m_{LE}(r) + \alpha_2 m_{HE}(r) + \alpha_3 m_{LE}(r) m_{HE}(r) + \alpha_4 {m_{LE}}^2(r) + \alpha_5 {m_{HE}}^2(r) \\ A_2(r) = \beta_0 + \beta_1 m_{LE}(r) + \beta_2 m_{HE}(r) + \beta_3 m_{LE}(r) m_{HE}(r) + \beta_4 {m_{LE}}^2(r) + \beta_5 {m_{HE}}^2(r) \end{cases} \quad (3)$$

Coefficients (α_k, β_k) are estimated by an experimental calibration procedure. Measurement data are acquired on calibration samples composed of both materials 1 and 2, of known thicknesses A_1, A_2, then used within a regression process to determine α_k, β_k. Notice that the exact knowledge of the X-ray spectra is not required, and the beam hardening effect is corrected thanks to calibration. This procedure, including the polynomial estimation, has to be proceeded for every pixel of the detector, unless they are corrected from spatial uniformity. Some authors prefer to use simulation to estimate the polynomials [8].

2.3 Graphical interpretation

In the axis set constituted by two measures *LE* and *HE*, the measurements corresponding to different thicknesses of a given material are located along a curve, which is a straight line under the bi-chromaticity hypothesis, of slope μ^{HE}/μ^{LE}. If the two energies are chosen in the photoelectric and Compton domain, $\mu^{HE} \approx \rho\beta_{HE}$, $\mu^{LE} \approx \rho\alpha_{HE} \cdot Z^m$, and the slope becomes $\beta_{HE}/\alpha_{LE} \cdot Z^m$. In polychromatic case, this line is slightly distorted. If we consider now the material basis, the space between the two axes can be squared by mixture of these two materials (figure 2, left). The point M corresponding to measures (m_{LE}, m_{HE}) is decomposed into material basis by points A_1 and A_2. Actually the angle between material basis axes is small, typically a few degrees.

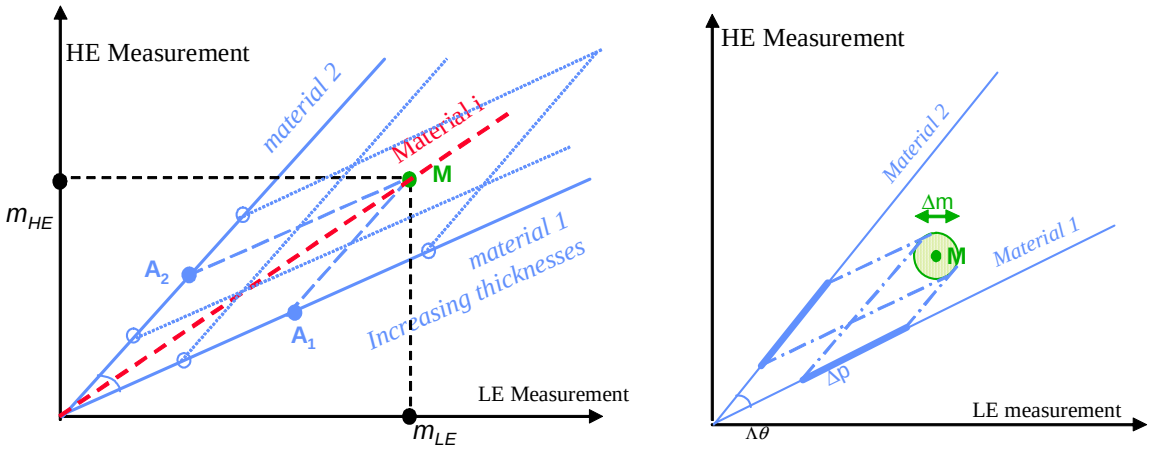

Figure 2: (*left)* representation of materials into the axis set composed of measures (m_{LE}, m_{HE}), (*right*) projection of uncertainty on material basis axes.

2.4 Noise and disturbances

The photon number, *N*, can be considered as a random variable having a Poisson distribution of parameter (thus variance) *N*. The variance of the log-measurement of the attenuation $m = -Log(N/N_0)$ is $1/N$, and the corresponding signal-to-noise ratio is given by: $SNR = -\sqrt{N}\,Log(N/N_0) = \sqrt{N} \cdot \mu \cdot T$.

Variance of the thickness estimate can be derived from the inverted linear system (1). From the decomposition on material basis, under the bi-chromatic assumption:

$T_1 = \alpha_1 m_{LE} - \beta_1 m_{HE}$ (with $\alpha_1 = \mu_2^{HE} / \Delta$, $\beta_1 = \mu_2^{LE} / \Delta$, and $\Delta = \mu_1^{LE} \cdot \mu_2^{HE} - \mu_1^{HE} \cdot \mu_2^{LE}$), we can deduce: $\sigma^2(T_1) = \alpha_1^2 \sigma^2(m_{LE}) + \beta_1^2 \sigma^2(m_{HE})$ so $\sigma^2(T_1) = \alpha_1^2 / N_{LE} + \beta_1^2 / N_{HE}$ where the photon number should be understood at the detector level (and similar equation for T_2). Once a typical thickness is given for each material, the standard deviation or the *SNR* can be computed as a function of the number of photons arriving on detector in *LE* and *HE*. This computation can be generalized to the polychromatic case [9]. To that photonic noise, we should add the electronic noise of the acquisition chain. On the graphical representation of Figure 2 (*right*), the uncertainty on measurement M is Δm, and is projected on material basis by two uncertainties Δp that depend on the angle between the two material axes. The more this angle is small the more noise is magnified by the decomposition. Notice that this angle depends on the chemical difference between materials, but also on the detection system itself, especially the separability of the two energy spectra.

In case of a 2D detector, the scatter radiation can not be ignored [10]. If the object is close to the detector, the scatter may reach 2 or 3 times the direct flux at 100 keV. When it is more distant, the scatter magnitude decreases and comes close to an offset. In any case, if the angle between the two material axes is small, the scatter has to be corrected. For medical applications, anti-scattering grids are often used, but the scatter elimination is not perfect. The technique of beam-stop grids consists to estimate numerically the scatter from a set of points (behind the beam-stop) and then to subtract it – but it requires an additional acquisition. For NDT, the use of beam-stop grids are often acceptable, except for moving objects in translation, or tomography. Nevertheless, emergent techniques allow to correct efficiently scatter in tomography [11].

It is important to notice that this correction has to be performed for the calibration samples and for the object under examination. Indeed, the scatter due to the object is specific to the shape of this object. It is eventually possible to learn it, when inspecting series of castings of same model. *LE* and *HE* scatters differ and have to be corrected separately. Finally, the influence of scatter inside the detector is not negligible, especially for flat panel.

3. System optimisation

3.1 General approach

Several choices have to be done when designing a dual-energy system. First the technique has to be specified, single exposure one with an energy-selective detector, or double exposure one by successive acquisitions. For that last one the design of the two energy spectra is critical, the energy switch is accomplished by voltage tuning associated to the addition of filters in front of the generator. The material basis has to be specified, and so are the calibration samples thicknesses. Some criteria exist to help these choices, but it is important to keep in mind that the optimum corresponds to a compromise, because the energy spectra shape is related to signal dynamic and noise. This compromise can eventually be non reachable. For instance, it is intuitive to choose the two energies as far from each other as possible, but a too low *LE* would induce a noisy, eventually non usable signal [12, 13, 14]. The criteria, that are discussed hereafter, are generally not sufficient to find an optimum and a constraint has to be added, related to the given system and operating conditions: constant dose, integration time, or global energy absorbed in the detector. This last one aims at benefiting of the whole detector's dynamic range. Other constraints have to be considered, related to geometry, practical considerations, and type of information required. Experiments can be used to help that design – if an easily tuneable rig is available, but the calibration step is fastidious. It is helpful to be provided with a simulation software

tool [8]. Sindbad software [15] developed by our laboratory has been used successfully for several system optimization [9].

3.2 Available criteria

A commonly used criterion is based on the Signal-to-Noise Ratio of the estimated thickness value, and allows to quantify the measure quality. From the noise model established at §2.4:

$$\sigma^2(T_1) = \frac{1}{\Delta^2}\left(\left(\mu_2^{HE}\right)^2\sigma^2(m_{LE}) + \left(\mu_2^{LE}\right)^2\sigma^2(m_{HE})\right) \qquad (4)$$

where, with bi-chromaticity hypothesis: $\sigma^2(m) = \frac{1}{N} = \frac{1}{N_0}\exp(\mu_1 T_1 + \mu_2 T_2)$ for each energy band.

We have to choose typical material proportions (T_1 , T_2), and a constraint to settle the number of photons (typically a constant $E_{absorbed}=E.N$). Then for each pair of possible energies (*LE*, *HE*) we can compute $\sigma^2(T_1)$ thus $SNR_1(E_{LE}, E_{HE})$, and we obtain a 2D-function of the two energy values, from which we determine an optimum. An example is shown in Figure 3 (*left*). The inspected object is a composite material consisting of glass fibre inside polyester binder, and the typical proportion is 0.1mm fibre in 5mm total thickness. The surface is plotted with isovalue lines. The optimum is reached at (20keV, 62 keV). The shape around the optimum is important, indicating the sensitivity of the *SNR* with regard to the energy.

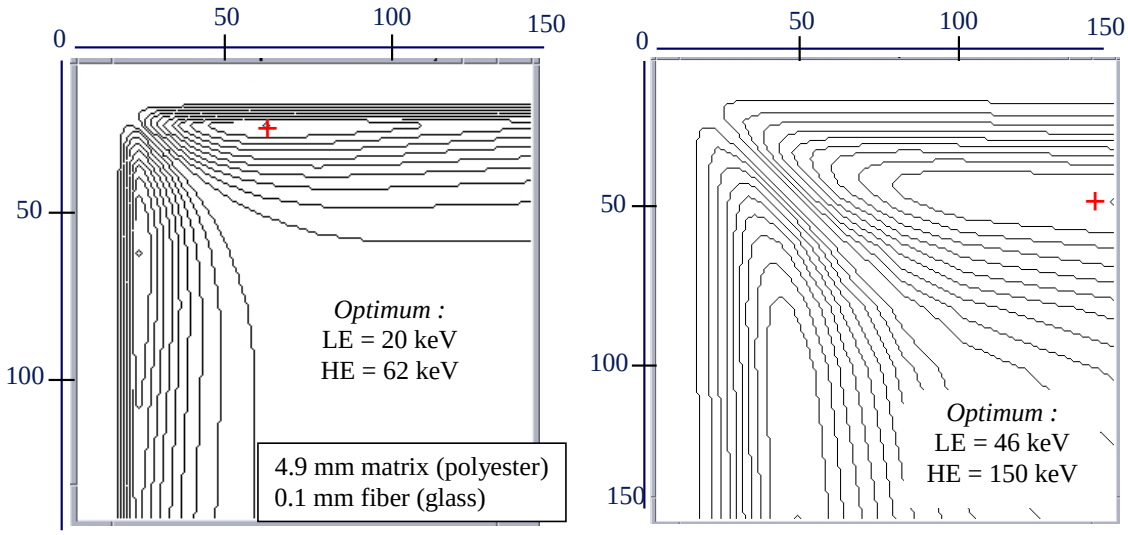

Figure 3: (*left) SNR* map for a composite material, isovalue lines representation, *(right*) Conditioning criterion for the same materials, isovalue lines.

Another criteria based on Contrast-to-Noise Ratio can be preferred to quantify measurement quality [7]. Contrary to *SNR*, it is a differential measure, and put emphasis on small variations in the mixture composition, which is useful when focusing on a constituting material which thickness ratio is low.

Now we consider the point of view of inversion stability. The numerical conditioning is the magnification factor of small perturbations of the linear system (3). It can be expressed by $cond = \|\bar{\mu}\| \cdot \left\|\bar{\mu}^{-1}\right\|$ where $\bar{\mu}$ is the attenuation matrix (attenuation coefficients) and $\|\ \|$ a matrix norm. The conditioning value is equal to 1 in the perfect case, and increases all the more than the system is badly conditioned. An example is shown in figure 3 (*right*), for the two materials glass/polyester. The map plotted is in fact (1/cond) with isovalue lines. The main difference between this stability criterion and the previous ones (*SNR* or *CNR*) is that

noise is not taken into account into the last one. It traduces an amplification factor to noise, and has to be combined with noise level. It can be shown that this numerical criterion is related to the angle between the two component material axes (figure 2).

3.3 Energy spectra design

Anyone of the above criteria allows to compute a theoretical optimum. The *SNR* one is usually chosen if typical material proportions can be defined. Notice that the shape of the optimization surface $\sigma(E_{LE}, E_{HE})$ is interesting, more or less flat around the optimum.

A first rapid estimate can be obtained using bi-chromatic hypothesis which leads to explicit expression of criteria as a 2D-function of (*LE*, *HE*), and using known values of attenuation coefficients. To get a more accurate optimum, especially if materials are closed in terms of attenuation properties, a simulation tool is required, based on detector and generator models, and realistic physical model of photon-matter interaction. Such a software can provide radiographs on which attenuation measurements, associated uncertainties, and thus the chosen criteria can be estimated.

The parameters to be determined are the high voltage of the generator, the acquisition time of *LE* and *HE* measures, and the filters (material and thickness) eventually placed in front of the tube – the system is clearly a multi-parametric one, arguing in favour of simulation rather than experiments. For double exposure technique, a K-edge filtration is often used. The principle consists in using a material presenting a K-edge around the needed cut-off energy (Cerium at 40 keV, Samarium at 47 keV, Holmium at 56 keV). Figure 4 illustrates this principle with a 200 µm thick Cerium filter. Of course practical reasons may intervene for the choice of filter thickness.

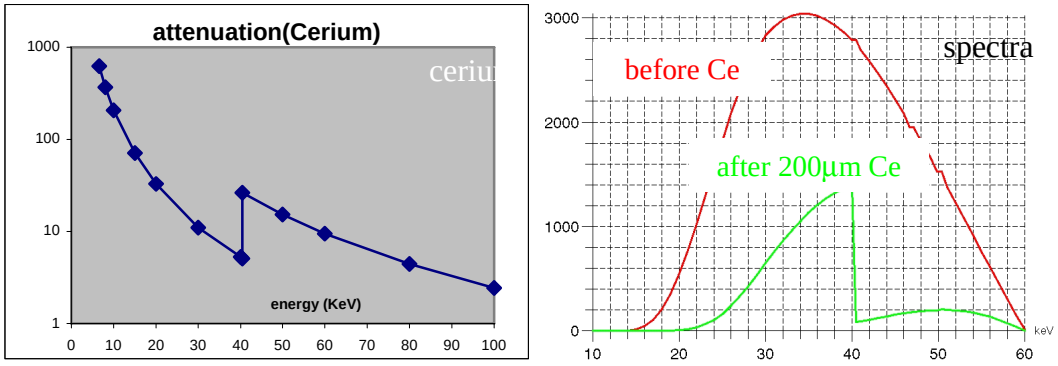

Figure 4: attenuation coefficient of Cerium, and its effect on the spectrum of a tube 60 KV.

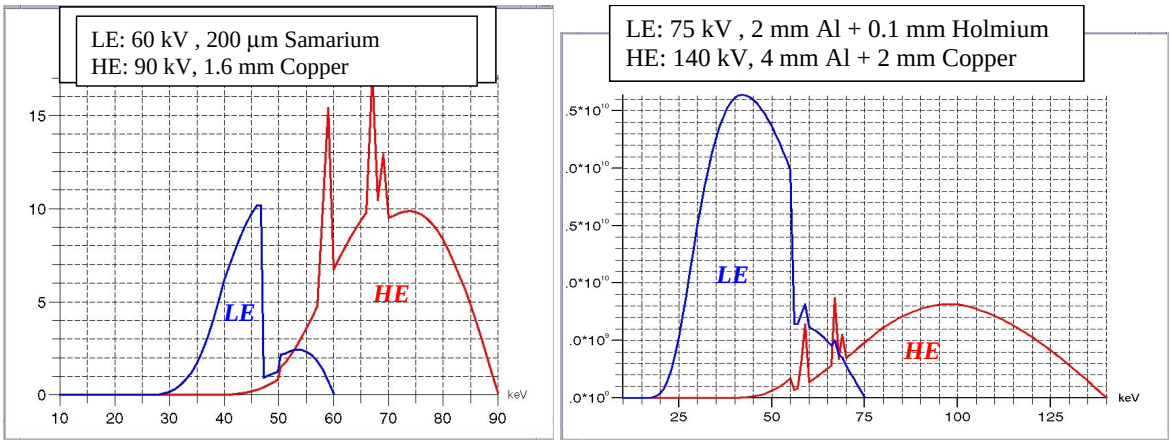

Figure 5: two examples of spectra for double exposure technique, using KV switch and K-edge filter.

Figure 5 shows two examples of spectra design with a good separability between *LE* and *HE* bands, devoted to double exposure technique, and both get by combining voltage switching and K-edge filtering technique. Represented spectra are those absorbed in the detector, after attenuation by typical material. Notice that the addition of too thick filters may reduce the spectrum peak too much, leading to choose a more powerful tube.

3.4 Absorbed Energy spectra and Detector

The criterion used to optimize the dual-energy system does not depend only on the mean energy peak, but also on the shape of the spectrum, and more precisely the separability of the two energy bands. Let us consider the following example of single exposure technique, obtained by simulation (figure 6). We use a standard generator 160 KV (mean energy 63 keV), and two detectors: a detector of sandwich type (leading to mean energy of absorbed energy spectra of *LE*=58 keV and *HE*=94 keV), and a detector of spectroscopic type, classifying the absorbed photons into two channels: 50-70 keV et 80-100 keV (the mean energy peaks are sensibly equal to the previous ones). In the representation given in §2.3, the two basis material, Plexiglas and aluminium, are separated by an angle of 6.2° for the sandwich-type detector, and 11.6° for the spectroscopic one. This corresponds to a magnification factor of noise for the second one which is only 60% of the first one.

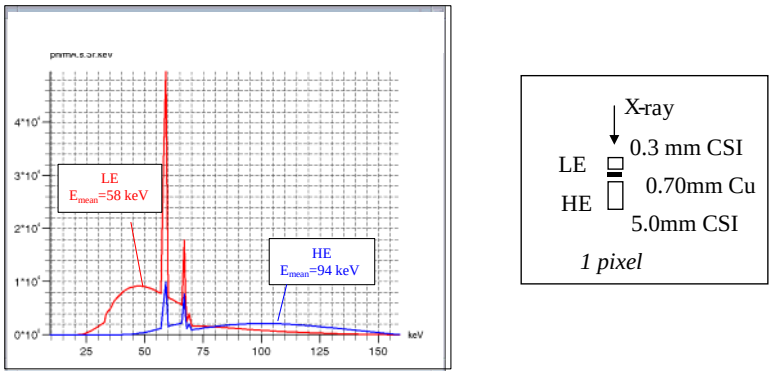

Figure 6: example of sandwich-type detector, showing a bad energetic separation.

3.5 Choice of material basis

If only two materials are constituent of the object, it is wishable to choose them as basis materials, as long as calibration samples of accurate thicknesses can be easily manufactured. If there are more than two constituent materials, and especially if their list is not precisely known (typical case of luggage), then a pair of materials have to be designed, close in terms of nature and thicknesses to the potentially present ones, in order to assure that the various disturbances (beam-hardening) are taken into account in a representative way. Notice that the validity of equation (2) can be checked for the chosen basis, and has been shown to be sometimes not perfect [16].

4. Applications

4.1 Material identification

In NDT applications, component materials are usually few and well-known. When only two material constituent are present, dual-energy radiography allows to identify them – more precisely to get images giving the thickness of each material at each pixel. We have seen

that it is possible only if the energy pair (*LE*, *HE*) leads to a separation higher than noise. In case of three component materials, the system is still solvable if an additional equation is provided, for instance the total object thickness, known or given by another sensor. Application of this technique in medical field has been proved to be efficient, especially for fat quantity estimation and bone densitometry, for which accurate quantitative information can be reached [10]. Application to food industry, particularly meat properties control [17] have been developed (material do not differ a lot from medical field). The challenge for food industry is to get an image by scanning the object on line, without interrupting the process flow of the factory. Single exposure technique is applied with a linear detector. The process has to provide contrasted images but not necessarily quantitative information.
A very promising application field concerns composite materials, increasingly used in various industries. Two types of information could be provided by dual-energy decomposition of composites: lack of binder (figure 7), and enhancement of fibre structure.

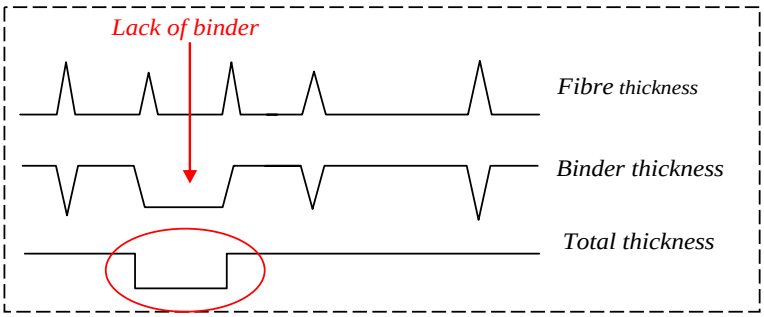

Figure 7: example of information from dual-material decomposition.

A complete study of optimized dual-energy protocol and process can be found in [7] for high heterogeneous material from insulation industry, composed of glass wool and injected binder. Another composite material, composed of carbon fibre inside a metallic matrix, is presented in figure 8. The total thickness image allows to get free from the structures present in the other images, and shows lack of binder.

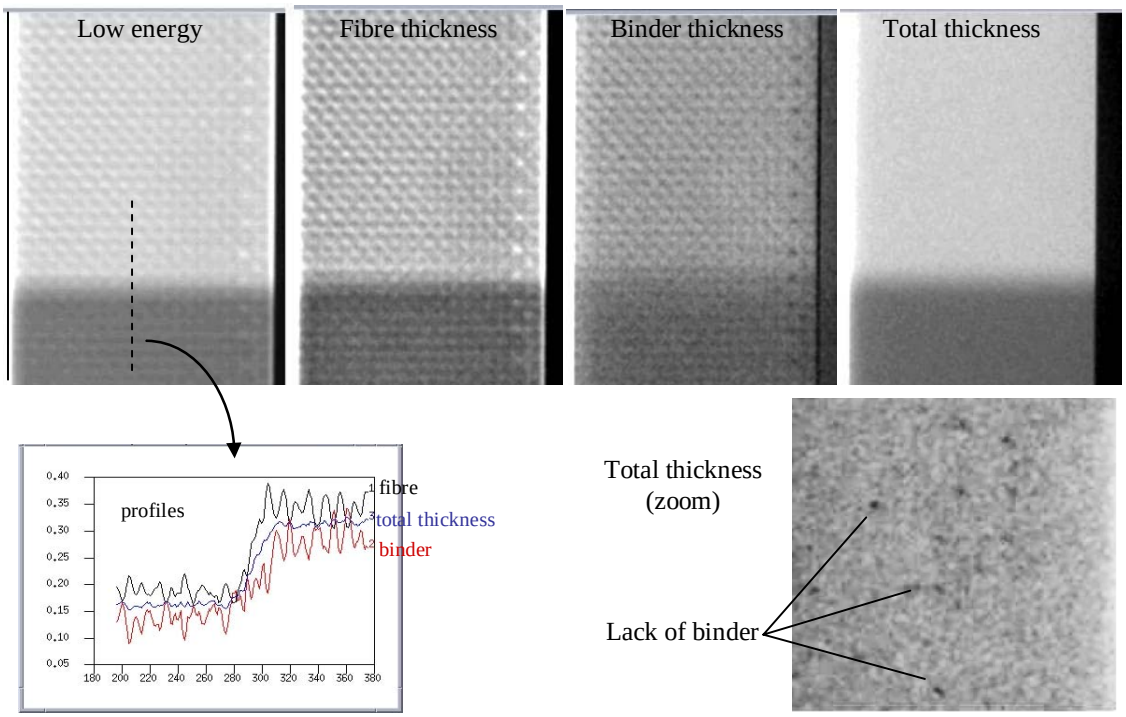

Figure 8: Composite material, carbon fibre and metallic binder (*thanks to EADS*)

If more than three materials are present, there is no more a unique decomposition, and for one pair of measurements several combination of thicknesses are possible. This lack of information is inherent in the radiographic projection, and tomographic techniques are required to overcome it (next §). Nevertheless it is possible in some cases to solve the ambiguity due to projection. The method proceeds by image segmentation and differential processes of the successive material layers. This algorithm is applied for luggage inspection [18]. The uncertainties are cumulating over the successive steps, and the final accuracy allows hardly to distinguish explosives from organic material. Notice that for luggage inspection [19] or waste drum control, the objective is to find a material – or a class of them – among a set of unknown ones. The problem is difficult and the searched material may be not distinguishable from the others.
An image of atomic number *Z* may be computed from the *Z* of the two basis material, but the accuracy on *Z* allows generally to classify material in only 2 or 3 *Z*-classes. Another use of dual-energy decomposition is to produce images with enhanced contrast. The principle, proposed in [3], consists in building a "projected" radiograph from two radiographs after decomposition on material basis. The goal being not as quantitative as thickness estimate (for bone densitometry for instance), the system needs are less strict.

4.2 Tomographic reconstruction

Let us consider a sequence of tomographic acquisition acquired with a dual-energy protocol. On each pair of radiograph (*LE*, *HE)* it is possible to apply dual-material decomposition and to get images of equivalent thickness (*A1*, *A2*). Then a reconstruction (in fact, two) can be performed and provides two volumes of equivalent percentage of material 1 and 2, $a_1(x, y)$ and $a_2(x, y)$. These two volumes may then be combined to get a density volume by: $\rho(x, y) = \rho_1 \cdot a_1(x, y) + \rho_2 \cdot a_2(x, y)$. Notice the processing order: first dual-energy decomposition, then reconstruction in two materials, and combination. Another solution would consist in reconstructing the two volumes before material decomposition. The first way is preferable, because it allows to integrate non-linearities correction (beam-hardening, ..) before reconstruction thanks to experimental calibration. But the second approach is sometimes used when the two sets of acquisition are not geometrically comparable at each image level. Laminography, that consists in the geometrical combination of several views with a translational motion, could also be combined with a dual-energy technique.

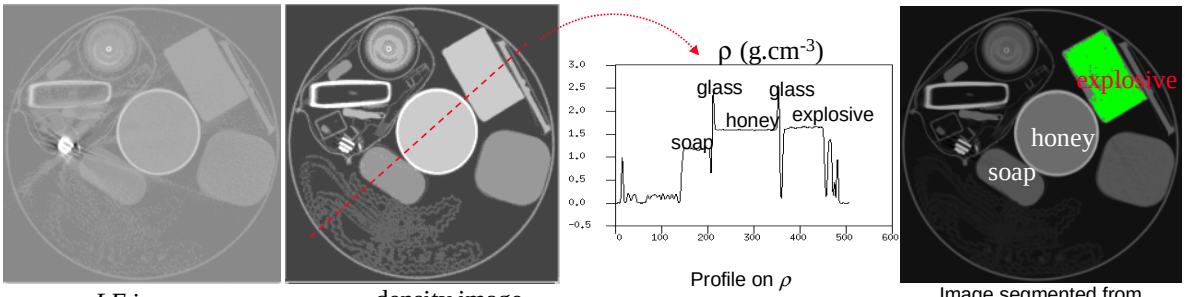

Figure 9: Dual-energy slice tomography on test luggage with explosive.

A reconstruction allows a classification, providing a volume of each component [20]. Such selective imaging of all components is required for correct modelling and understanding of the mechanical properties of heterogeneous material. It may be necessary for composites inspection [21]. Indeed, the detection of lack of binder can be achieved by radiography, but the characterization of the 3D-structure fibres requires tomography. Due to the dimension of the fibres, a micro-CT has to be applied [22, 23], and combined with a dual-energy

protocol would provide selective volumetric imaging. In case of explosive detection inside luggage, dual-energy tomography should allow to distinguish explosives from most of materials, but requires to interrupt the luggage flow on the conveyor belt. Figure 9 shows an example of explosive detection thanks to ρ and Z information, density ρ information being not sufficient when used alone. Application to radioactive waste drum control has also been tested [24], figure 10.

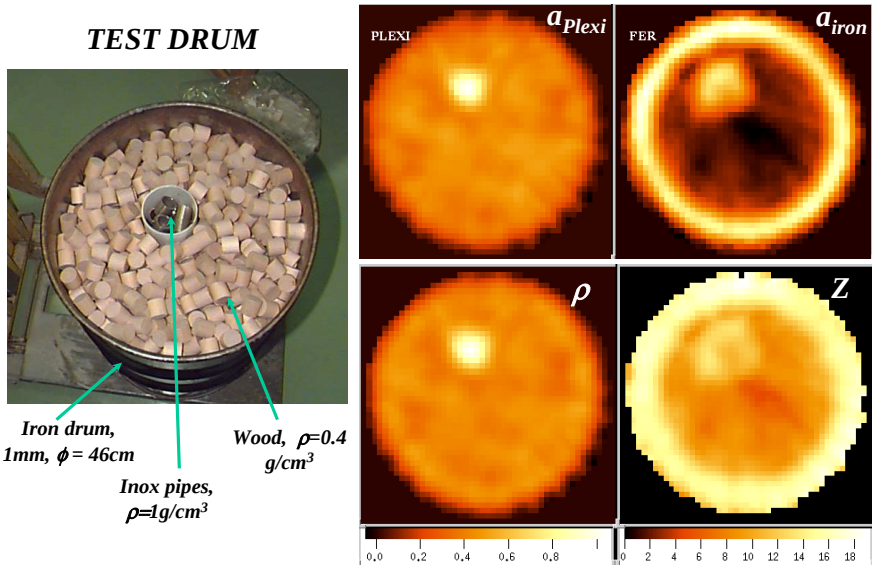

Figure 10: Dual-energy tomography on test drum.

4.3 Multi-energy techniques

Perion et Maitrejean have developed a method that generalized the conventional dual-energy method [25]. The target application is explosive detection, and more generally the chemical identification of materials. From the authors, the achieved accuracy is 0.5% on attenuation coefficient. The method is implemented in the commercialized system "Excalibur". The acquisition requires six successive exposures, the energy switch being performed at the generator level – consequently the system is difficult to tune and its maintenance complex. Other methods have been proposed for the identification of organic substance [26]. The adaptation of the multi-energy approach to spectroscopic-type detector, providing with a single exposure different energy channels with a good energy accuracy, should open very promising applications.

Conclusion

Dual energy techniques can be very useful for industrial NDT applications. The complexity of the problem depends on the number of constituent materials, the prior knowledge about them, and the information required (thickness or other). Constraints should be considered, especially acquisition geometry and time limit. Several techniques are available, single or double exposure ones, with convenient generator and detector. The system has to be optimized thanks to some criteria, the parameters concerning the two energies spectra design, but also the material basis, which is not obvious if more than two components are present. The target system is specified by the description of the generator and detector, the acquisition protocol, and the polynomials function for dual energy decomposition. The final benefit depends on the closeness of the two materials, the measurement noise and the noise magnification factor related to the system (spectra of generator, or detector). Dual-energy techniques, associated to tomography or laminography should provide promising solutions

addressing new applications in the future. The use of emergent detectors, as semi-conductor spectroscopic one, should provide opportunity to develop new multi-energy technique.

References

[1] L.Verger, JP.Bonnefoy, F.Glasser, P.Ouvrier-Buffet, *New developments in CdTe and CdZnTe detetors for X and gamma-ray applications, Journal of electronic materials*, vol 26, n°6, pp 738-44, 1997.

[2] R.E. Alvarez et A. Macovski, *Energy selective reconstructions in X-ray computerized tomography*, *Phys. Med. Biol*. Vol. 21, PP. 733-744, 1976.

[3] L.A. Lehmann, R.E. Alvarez, A. Macovski, W.R. Brody, N.J. Pelc, S.J. Rieder, A.L. Hall, *Generalized image combinations in dual KVP digital radiography*, *Med. Phys* 8(5), Sept 1981

[4] K-Shih Chuang and H.K. Huang, *Comparison of four dual energy image decomposition methods*, Phys. Med. Biol., 1988, Vol.33, N°4, 455-466.

[5]H.N.Cardinal, A.Fenster, *An accurate method for direct dual-energy calibration and decomposition*, Med Phys 17 (3), pp 327-341, May/june 1990.

[6] K.Goh, S.Liew, B.Hasegaw, *Correction of energy-dependant systematic errors in dual energy X-ray CT using a basis material coefficients transformation method*, IEEE Trans.Nucl.Sci vol 44, n°6, dec.1997.

[7] JM.Letang, N.Freud, G.Peix, *Signal-to-noise ratio criterion for the optimization of dual-energy acquisition using virtual x-ray imaging : application to glass wool*, Journal of elec. imaging, 13:436-49, 2004.

[8] JM.Letang, N.Freud, G.Peix, *Optimal calibration via virtual X-ray imaging for dual-energy techniques: application to glass wool*, Proc.SPIE vol.5132, pp 422-32, 2003.

[9] L.Hervé, C.Robert-Coutant, JM.Dinten, L.Verger, V.Comparat, *Optimization of X-ray Spectra for bone mineral density and body composition measurement. Theoretical study and experimental validation.* Proc.SPIE Annual Meeting, Seattle 2002.

[10] JM.Dinten, C.Robert-Coutant, M.Darboux, *Dual-energy X-rays absorptiometry using a 2D digital radiography detector. Application to bone densitometry*, SPIE Medical Imaging 2001.

[11] J.Rinkel, F.Esteve, JM.Dinten, *Evaluation of a physical based approach of scattered radiation correction in cone beam CT for NDT applications*, 9th ECNDT , Berlin 2006.

[12] A.Talbert, R.Brooks, D.Morgenthaler, *Optimum energies for dual energy CT*, Phys.Med.Biol. 1980, vol25, n°2, pp 261-269.

[13] R.Seppi, *A comparison of noise and dose in conventional and energy selective computed tomography*, IEEE Trans. on Nuclear Science 26(2), pp 2853-56, 1979.

[14] J.Sorenson, P.Duke, S.Smith, *Simulation studies of dual-energy x-ray absorptiometry*, Med.Phys., 16(1), Jan 1989

[15] R. Guillemaud, J. Tabary, P. Hugonnard, F. Mathy, A. Koenig, A. Glière, *Sindbad: a multi-purpose and scalable X-ray simulation tool for NDE and medical imaging*, PSIP 2003, Grenoble, France, 2003.

[16] E.Gingold, B.Hasegawa, *Systematic bias in basis material decomposition applied to quantitative dual-energy x-ray imaging*, Med.Phys.19(1), pp. 25-33, 1992.

[17] C.Kroger, C.Bartle, J.West, *Non-invasive measurement of wool and meat properties*, Insight Vol 47 No 1 January 2005

[18] R.Eilbert, K.Krug, *Aspects of image recognition in Vivid technology's dual-energy x-ray system for explosive detection*, Proc. of SPIE, vol.1824, 1992.

[19] R.Macdonald, *Design and implementation of a dual-energy X-Ray imaging system for organic material detection in an airport security application*, Proc. of SPIE Vol.4301 (2001) .

[20] J.Coenen, J.Mass, *Material classification by dual-energy computerized X-ray tomography*, in Int.Symp. on Comp.Tomography for indust. applications, DGZfp, june 1994.

[21] P.Rizo et C.Robert-Coutant, *Dual-energy tomography for ceramics and composites materials*, Int.symp.on CT for industrial applic., June 1994 in Berlin, DGZfP, pp.128-135, 1994

[22] E.Cornelis, A.Kottar, A.Mohammed, H.Degischer, *X-ray computed tomography characterising carbon fiber reinforced composites*, Proc. of the ICCM-14 Conference, San Diego, Calif., July 14-18th, 2003

[23] P.Schilling and All, *X-ray computed microtomography of internal damage in fiber reinforced polymer matrix composites*, Composites Science and Technology 65 (2005) 2071-2078

[24] C.Robert-Coutant, V.Moulin, R.Sauze, P.Rizo, JM.Casagrande, *Estimation of the matrix attenuation in heterogeneous radioactive waste drums using dual-energy computed tomography*, Nuclear Ins. & methods in Physics research, A 422, pp 949-956, 1999.

[25] S.Maitrejean, D.Perion, D. Sundermann, *Non destructive chemical identification using an X-ray transmission function obtained with the multi-energy method*, Proc. SPIE Vol. 3446, pp134-152 (1998).

[26] S.Naydenov and V.Ryzhikov, *Multi-energy techniques for radiographic monitoring of chemical composition*, Nucl.Inst. & methods in Phys.Res. A 505 (2003) 556-558.